Gold Fingers: 3D Targets for Evaluating Capacitive Readers

Sunpreet S. Arora, Anil K. Jain, *Life Fellow, IEEE,*
and Nicholas G. Paulter Jr. *Fellow, IEEE*

***Abstract*—With capacitive fingerprint readers being increasingly used for access control as well as for smartphone unlock and payments, there is a growing interest amongst metrology agencies (e.g. the National Institute of Standards and Technology) to develop standard artifacts (targets) and procedures for repeatable evaluation of capacitive readers. We present our design and fabrication procedures to create conductive 3D targets (gold fingers) for capacitive readers. Wearable 3D targets with known feature markings (e.g. fingerprint ridge flow and ridge spacing) are first fabricated using a high-resolution 3D printer. A sputter coating process is subsequently used to deposit a thin layer (~300 nm) of conductive materials (titanium and gold) on 3D printed targets. The wearable gold finger targets are used to evaluate a *PIV* certified single-finger capacitive reader as well as small area capacitive readers embedded in smartphones and access control terminals. Additionally, we show that a simple procedure to create 3D printed spoofs with conductive carbon coating is able to successfully spoof a *PIV* certified single-finger capacitive reader as well as a capacitive reader embedded in an access control terminal.**

***Index Terms*—3D fingerprint targets, capacitive reader evaluation, sputter coating, 3D spoofs.**

(a) (b)

Fig. 1. 3D targets for evaluating capacitive readers. (a) Sample gold finger target, and (b) 2D impression of the gold finger in (a) captured using a *PIV* certified 500 ppi single-finger capacitive reader.

I. Introduction

There are, at present, over 2 billion smartphone users[1] worldwide, and it is estimated that the user base will grow to around 2.66 billion by 2019, *i.e.*, within the next few years, over one-third of the world population will be using a smartphone [2]. Following the introduction of fingerprint-based smartphone unlock and payment technology by major vendors, a large number of smartphone users now have access to smartphones equipped with fingerprint readers. One of the primary reasons for the use of fingerprint-based authentication, in particular, and biometrics in general, in smartphones is their ease of use and higher security compared to traditional passcodes. About 29% of the smartphones shipped in 2016 had a fingerprint reader; this number is expected to more than double in the next two years [3]. It is estimated that in 2018, two out of every three shipped smartphones will have a fingerprint reader [3]. Furthermore, the number of smartphone users employing Near Field Communication (NFC) technology for mobile payments is expected to triple from about 54 million in 2016 to 166 million in 2018 [4].

The embedded fingerprint readers in most smartphones, including those from major vendors, e.g., [5], [6], and [7], use capacitive sensing. Capacitive readers typically consist of a capacitive sensor array (e.g. silicon, flex), where each element of the array is a mini-sensor in itself that senses the capacitance difference between ridges and valleys [8]. The sensor array acts as one plate of a parallel-plate capacitor, the electrically conductive dermal layer of the finger skin acts as the other plate, and the non-conductive epidermal layer acts as a dielectric. Most capacitive readers use active sensing, i.e., they apply a small voltage to the skin to induce an electric field between the finger and the sensor array. The induced electric field follows the pattern of the ridges in the dermal layer and the voltage difference with respect to reference voltage is used to sense the fingerprint. Capacitive readers typically have a small form factor, with the sensing area between 0.2-2 cm^2, to keep the reader cost low. The small form factor coupled with low cost makes capacitive readers suitable for embedding in mobile devices including smartphones, laptops and tablets (see Fig. 2). In addition, capacitive readers have also been embedded in standalone terminals for access control.

S. S. Arora is with the Risk and Authentication Products Group at Visa Inc., Foster City, CA 94404. Email: sunarora@visa.com.

A. K. Jain is with the Department of Computer Science and Engineering, Michigan State University, East Lansing, MI 48824. E-mail: jain@cse.msu.edu.

N. G. Paulter Jr. is with the National Institute of Standards and Technology (NIST), Gaithersburg, Maryland 20899. Email: paulter@nist.gov.

[1]The term *smartphone* refers to cellular telephones with integrated computer and other features not originally associated with telephones, such as an operating system, web browsing and the ability to run software applications. [1]

(a) (b) (c) (d)

Fig. 2. Examples of capacitive fingerprint readers embedded in (a) and (b) smartphones, (c) a tablet and (d) an access control terminal.

TABLE I
COMPARISON OF THE MECHANICAL AND ELECTRICAL PROPERTIES OF THE HUMAN SKIN WITH GOLD FINGERS FABRICATED USING THE TWO PRINTING MATERIALS.

Property	**Description/Benefit**	**Human Skin [9] [10] [11] [12]**	**TangoBlackPlus FLX980 [13]**	**FLX 9840 -DM [14]**
Hardness (Shore A)	Proper presentation on the reader platen	20-41	26-28	35-40
Tensile Strength (MPa)	Durability for repeatable operational evaluation	5-30	0.8-1.5	1.3-1.8
Elongation at Break (%)	Pertinent distortion on contact with the reader platen	35-115	170-220	110-130
Electrical Resistance (MΩm)	Resistance to flow of electric charge	1-2	0.0005-0.001*	0.0005-0.001*

* Approx. measurements obtained using a multimeter.

A. Prior Work

Existing fingerprint reader evaluation standards (*PIV* [15] and *Appendix F* [16]) recommend the use of 2D or 3D targets for testing the imaging capabilities of readers. The standard practice followed by most fingerprint vendors is to use 2D targets for this purpose. However, 2D targets are inadequate from the operational perspective, e.g., to test the impact on quality of the acquired image due to differences in finger placement, pressure and distortion on the reader platen.

In our previous work [17], we designed and fabricated 3D targets for operational evaluation[2] of single-finger optical fingerprint readers. We projected 2D calibration patterns with known features, e.g., sine gratings generated with predefined orientation and spacing, synthetic fingerprints with known fingerprint type, ridge flow, ridge spacing and minutiae points, onto a generic 3D finger surface to create electronic 3D targets. A state-of-the-art 3D printer was used for physical fabrication of the 3D targets with materials similar in hardness and elasticity to the human skin. We showed that the 3D target synthesis and fabrication process was able to reproduce calibration patterns with high fidelity on both electronic (virtual) and physical 3D targets. We also demonstrated that the fabricated 3D targets can be utilized for evaluation of three different single-finger optical readers.

Subsequently, in [18], we extended the single-finger target generation method to create whole hand 3D targets for evaluating contact-based and contactless slap fingerprint readers. We segmented 3D finger surfaces pertaining to each of the four fingers and the thumb from a 3D hand surface and projected calibration patterns onto each finger surface to generate electronic 3D whole hand target. We used a high-resolution 3D printer to manufacture physical 3D hand target with materials that were similar in mechanical properties to the human skin as well as compatible for imaging with a variety of optical fingerprint readers. Furthermore, the generated targets were used to perform evaluation of three contact-based slap readers and one contactless slap reader.

B. Objective

Although suitable for use with optical readers, the 3D targets designed in [17] and [18] were not compatible with capacitive readers as the fabrication materials available to print the 3D targets (UV-curable rubber-like polymeric materials: TangoBlackPlus FLX980, FLX 9840-DM, TangoPlus FLX930 and FLX 9740-DM[3]) are non-conductive. State-of-the-art high-resolution 3D printers only support printing with limited rubber-like polymer materials that are electric insulators.

Given that a large number of capacitive fingerprint readers are being used in consumer and access control appli-

[2]The term *evaluation* is used in the paper to refer to the operational (black-box) testing of imaging capabilities of readers using standard artifacts (targets).

[3]The naming of companies and products here does not imply endorsement or recommendation of those companies or products by the authors or the organizations they represent.

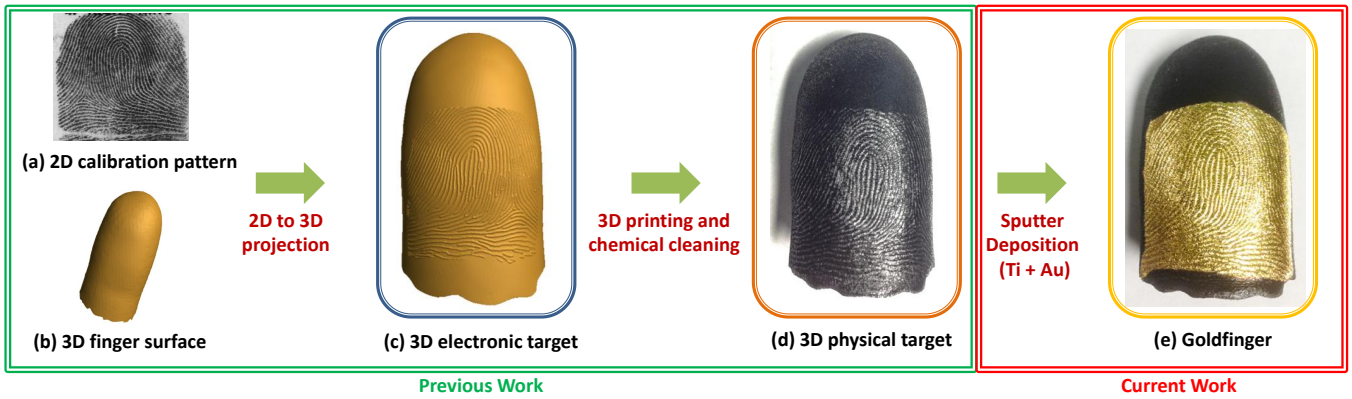

Fig. 3. Main steps involved in creating a gold finger given a 2D calibration pattern and a 3D finger surface. (a)-(c) A 2D calibration pattern is projected onto a 3D finger surface to generate a 3D electronic target and (d) 3D physical target is fabricated from the electronic target in (c) using a high-resolution 3D printer [17]. (e) A thin layer of titanium (30 nm) and gold (300 nm) is sputter coated on the 3D physical target to generate conductive 3D target (gold finger).

cations, e.g., smartphone unlock and payments, metrology agencies, e.g, the National Institute of Standards and Technology (NIST), are interested in the design and development of standard artifacts (targets) and procedures for repeatable evaluation of capacitive readers[4] in a controlled manner (see Section IV-A). To that end, the objective of this research is to design and fabricate 3D targets for evaluating capacitive readers.

C. Contributions

In this paper, for the first time, we report the design and fabrication of 3D targets suitable for imaging with single-finger capacitive fingerprint readers (see Fig. 1; also see Table I for the mechanical and electrical properties of the human skin and the fabricated 3D targets). We first use the method in [17] to create 3D targets with materials similar in hardness and elasticity to the human skin[5] (Fig. 3(a)-(d)). We then use a sputter deposition technique (Fig. 3(e)) to coat the surface of 3D targets with thin layers of conductive materials (titanium (Ti) + gold (Au)). We refer to the Ti-Au coated 3D targets as *gold fingers*. We show that the sputter deposition of 30 nm Ti followed by 300 nm Au does not alter the features etched on the 3D targets for any loss in comparison accuracy. Furthermore, we show that the coated 3D targets can be imaged with two different types of capacitive fingerprint readers: small area readers (~0.5 cm×0.9 cm) designed for smartphones, and relatively larger area (~1.3 cm×1.8 cm) readers embedded in access control terminals. In summary, the contributions of this paper are as follows:

- Developed a method to coat 3D printed targets with a thin layer of appropriate conductive materials (~300 nm thickness) for imparting electrical conductivity to the targets and enabling sensing by capacitive readers.

[4]Repeatable evaluation of readers is an important requirement to benchmark different readers based on their imaging capabilities.

[5]In our experiments, hardness greater than 50-60 on the Shore A scale and elongation at break larger than 300% were found to adversely impact the quality of the presented calibration pattern on capacitive readers.

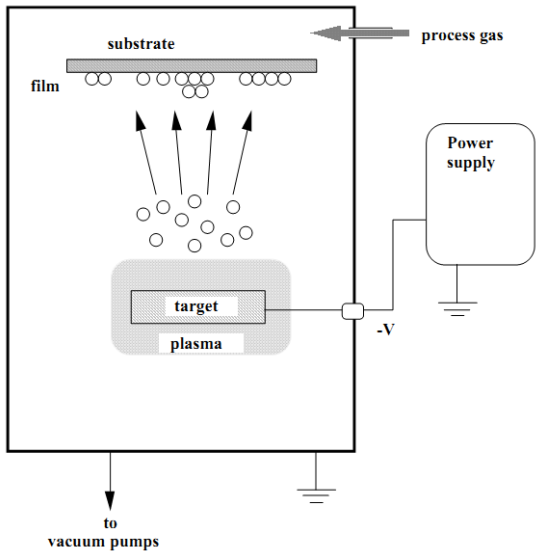

(a)

(b)

Fig. 4. DC sputter deposition to coat the 3D targets, fabricated using a high-resolution commercial 3D printer, with thin layers of conductive materials. (a) Simplified representation of the DC sputtering process (image reproduced from [19]), and (b) the Denton Vacuum DC sputtering system [20] used for DC sputtering. Conductive material from the cathode target (titanium (Ti) and gold (Au) used here) is deposited on the anode substrate (3D target) using Argon (Ar) as the process gas.

- Quantitative evaluation to show that the coating process does not impact fingerprint features extracted from the 3D printed targets for any loss in the comparison accuracy. In other words, the coating preserves the fingerprint features used in fingerprint matching.
- Demonstrated that the coated targets can be used for evaluating standalone single-finger capacitive readers, as well as readers embedded in access control terminals and smartphones.
- Developed conductive 3D spoofs to evaluate spoof vulnerability of capacitive readers.

II. Sputter Coating 3D Targets

As mentioned earlier, state-of-the-art 3D printers, e.g. Stratasys Objet Connex350 used in our study [21], support only limited printing materials that do not possess electrical conductivity. To impart conductivity to the printed 3D targets, DC sputter deposition technique [19] is used to coat the target surface with thin layers of conductive materials. Fig. 3 illustrates the main steps involved in generating a gold finger given a 2D calibration pattern and a 3D finger surface.

Sputter deposition is one of the most popular techniques for depositing thin conductive films on insulators and semiconductors [22]. It is widely used in the semiconductor industry to deposit thin films on integrated circuit components, for anti-glare coatings on glass in optics, and to deposit thin metallic layers on CDs, DVDs and solar cells [22]. Different types of sputter deposition methods, e.g., ion beam sputtering, DC sputtering, RF sputtering, can be used depending on the characteristics of the substrate and the target material to be deposited, and the desired coating thickness. Here, we use DC sputtering because this method is both suitable and efficient for applying extremely thin conductive material coatings (~300 nm) on 3D fingerprint targets.

A. DC Sputtering Process

Fig. 4 (a) illustrates the DC sputtering process [19]. The sputtering chamber is first evacuated to remove water vapour and atmospheric gases that could interfere with the sputtering process. The sputtering target made of the conductive material to be deposited (e.g. silver (Au), Copper (Cu), or Gold (Au)) is placed at the cathode, and the substrate (3D target) on which the thin layer has to be deposited is placed at the anode. A process gas (typically Argon (Ar)) is then added to the vacuumed chamber at a pre-specified pressure, typically between 1-100 mTorr. A negative potential bias that is sufficient for electron emission from the sputtering target (generally between 500-5000 volt (V) DC) is applied to the cathode. Electrons emitted from the target due to this negative bias strike the molecules of the process gas in the neighborhood of the cathode (sputtering target) and produce positively charged process gas ions. The generated positive gas ions travel towards the cathode due to the negative potential bias. When the process gas ions collide with the cathode (sputtering target), their kinetic energy is transferred to the target resulting in the ejection of sputtering material atoms. The ejected material atoms move towards the anode where they deposit to form a thin layer on the substrate surface.

B. Choice of Sputtering Materials

One of the major design considerations in choosing the appropriate material for imparting conductivity to the 3D printed targets is the durability of the conductive material coating. Coating durability is assessed in terms of (i) tolerance to oxidation or tarnishing and (ii) resistance to abrasion due to repeated use of the 3D target. We investigated coating durability for a number of different sputtering materials and their combinations (see Table II).

We initially sputter coated metals such as silver (Ag), copper (Cu), and chromium (Cr) on the 3D fingerprint targets over titanium (Ti) coating (see, e.g, Figs. 5 (a) and (b)). Titanium (Ti) was first sputter deposited on the 3D printed samples because it has good adhesion/binding properties to the 3D printing material as well as metals. Although coatings of the aforementioned metals were found to impart sufficient conductivity for the 3D targets to register on capacitive readers, the metal coatings reacted with atmospheric gases and water vapours over time and tarnished (e.g. due to formation of copper carbonate ($CuCO_3$) and chromium oxide (Cr_2O_3)) the 3D target surface. This rendered the 3D targets unusable with capacitive readers because of the loss of electrical conductivity.

We also attempted to coat transparent conductive oxides, e.g, tin (Sn) doped indium oxide (ITO) [23], zinc (Zn) and Al doped indium oxide (IZAO) [24], and Sn, Zn and Al doped indium oxide (IZATO) [25] on 3D printed targets using DC sputtering (see, e.g, Fig. 5 (c)). The primary advantage of using transparent conductive oxide coatings over metallic coatings is their high transparency which does not significantly impact the underlying optical properties [26] of the 3D targets. This way, the same target can potentially be used for optical and capacitive readers. However, the wear and tear (abrasion resistance) of conductive oxide coatings was found to be inadequate for repeatable evaluation of capacitive readers over time. In our tests, the coatings were found to wear out after taking about five to ten impressions of the coated targets with capacitive readers.

We hypothesized that the low abrasion resistance of conductive oxide coatings is due to the low receptivity of the 3D target surface to conductive oxide coatings. To address this issue, two possible alternatives were explored: (i) plasma pre-treatment before sputtering and (ii) heat curing post-treatment after sputtering. Pre-treatment of the 3D target surface with high energy plasma for a short duration of time before sputtering ITO was found to impact the calibration patterns etched on the 3D surface. High temperature annealing, post DC sputtering, to cure the coating physically deformed the target because the 3D printing materials were found to be sensitive to high temperatures ($\geq 60^\circ$ C). Further investigation is required to identify a procedure to ensure abrasion resistance of transparent conductive oxide coatings.

We also experimented with the application of a thin layer (50 nm) of PEDOT:PSS colloidal solution on a 3D target using spin coating (at 2000 rpm). However, (i) the coating was non-uniform and (ii) the conductivity of the coated target was inadequate for registration on capacitive readers. Exploration of methods to improve the conductivity of PEDOT:PSS solution

(a) (b) (c)

Fig. 5. 3D fingerprint targets coated with (a) a thin layer (300 nm) of silver (Ag), (b) a thin layer (300 nm) of copper (Cu), over a thin layer (30 nm) of titanium (Ti); (c) 100 nm coating of tin (Sn) doped indium oxide (ITO). The targets in (a) and (b) were printed using the Stratasys Objet Connex350 with TangoBlackPlus FLX980 [13] and the target in (c) was printed with TangoPlus FLX930 [13]. Targets coated with other conductive transparent oxides are not shown here because they are visually similar to (c).

TABLE II
QUALITATIVE COMPARISON OF SPUTTER COATED THIN FILMS ON 3D TARGETS.

Coating Material	Coating Thickness	Conductivity [1]	Tolerance to Oxidation (Tarnishing) [2]	Resistance to Wear and Tear [3]
Ti + Au	30 nm + 300 nm	Adequate	High (doesn't tarnish)	High
Ti + Ag	30 nm + 300 nm	Adequate	Low (~1 week)	High
Ti + Cu	30 nm + 300 nm	Adequate	Low (~2 weeks)	High
Cr	300 nm	Adequate	Low (~1-2 days)	High
ITO	100 nm	Adequate	High (doesn't tarnish)	Low (5-10 uses)
IZAO	300 nm	Adequate	High (doesn't tarnish)	Low (5-10 uses)
IZATO	300 nm	Adequate	High (doesn't tarnish)	Low (5-10 uses)

[1] Conductivity at working frequency for appropriate registration on capacitive readers.
[2] Time period before the target tarnishes in air.
[3] Number of uses before wear and tear makes the target unusable with capacitive readers.

TABLE III
PARAMETER SETTINGS FOR TI+ AU DC SPUTTERING.

Parameter	Value
Ar gas pressure	4 mTorr [1]
Power source	125 W [2]
Ti sputtering rate	0.21 nm/s
Ti layer thickness	30 nm [3]
Ti sputtering time	2.4 min
Au sputtering rate	1.1 nm/s
Au layer thickness	300 nm
Au sputtering time	5 min

[1] milliTorr
[2] Watts
[3] nanometers

by doping it with solvents, e.g, DMSO (e.g., [27], [28]) before its application on 3D targets will be done in future.

Based on this extensive experimentation, gold (Au) was chosen for coating 3D targets because it is an inert metal that does not react with atmospheric gases and Au coating has relatively high abrasion resistance. Table II lists the advantages and disadvantages of applying different conductive coatings on 3D fingerprint targets using DC sputtering.

C. Sputtering Ti+Au

The Denton Vacuum Desktop Pro [20], a compact, high vacuum sputtering system, is used for DC sputtering (see Fig. 4 (b)). The sputtering system has a rotary platform where the 3D target to be coated is placed and rotated in order to uniformly coat the substrate surface with the conductive material. Directly placing the 3D targets on the rotary platform is unstable, so we fabricated a stable 3D mount to hold the 3D target before placing them on the platform. The 3D mount is designed in Meshlab [29] by combining a generic 3D model of a finger with a rectangular base with dimensions of 35 mm $\times$ 37 mm $\times$ 10 mm (see Fig. 6 (a)). The mount is printed using the Stratasys Objet Connex350 3D printer with the rigid opaque white material, VeroWhite [13] (Fig. 6 (b)). The 3D target is placed on this mount before sputtering. Furthermore, the 3D target region without etchings is covered with tape to only sputter target material on regions containing the etched pattern, e.g, friction ridge pattern. This tape is removed after

(a) (b) (c)

Fig. 6. 3D mount fabricated (using Stratasys Objet Connex350) to hold a 3D target for stable placement on the sputtering system's rotary platform. (a) Electronic 3D model, (b) 3D printed physical model and (c) 3D fingerprint target on the mount shown in (b) after gold coating.

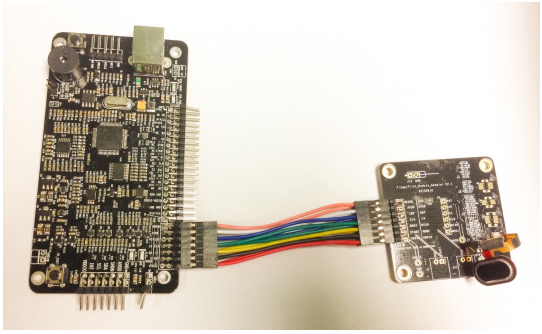

(a)

(b)

Fig. 7. Sample impressions (b) of a gold finger captured using the embedded capacitive reader designed for smartphones (a). Each impression is approx. 70×120 pixels.

sputtering to obtain the coated 3D target analogous to that shown in Fig. 1 (a).

Table III lists the experimental parameters used for DC sputtering. High purity (>99%) thick gold (Au) and titanium (Ti) sputtering targets with 2.0" diameter × 0.125" [30] [31] are used. Argon (Ar) is used as the process gas at a pressure of 4 mTorr and a power source of 125 W is used. 30 nm of Titanium (Ti) is first sputter deposited on the 3D targets because it has good adhesion/binding properties to the 3D printing material as well as gold (Au). This is followed by sputter deposition of 300 nm of Au[6] on the 3D targets. The sputtering rates for Ti and Au at 125 V negative bias are 0.21 nm/s and 1.1 nm/s, respectively. At these sputtering rates, it takes about 2.4 minutes to sputter 30 nm Ti and about 5 minutes to sputter 300 nm Au. The estimated in-house cost of sputter coating each 3D target with 30 nm Ti and 300 nm Au is approximately US $2. The cost to generate a physical 3D target is approximately US $10, so the total estimated cost to fabricate a gold finger is about US $12.

TABLE IV
SIMILARITY SCORES BETWEEN 500 PPI PLAIN IMPRESSION OF 3D TARGETS CAPTURED BY THE OPTICAL READER TO 500 PPI PLAIN IMPRESSION OF THE CORRESPONDING SPUTTER COATED GOLD FINGERS CAPTURED BY THE CAPACITIVE READER. VERIFINGER 6.3 [33] WAS USED FOR GENERATING SIMILARITY SCORES. THE THRESHOLD ON SCORES @FAR = 0.01% IS 33.

Source Fingerprint (NIST SD4)	S0005	S0010	S0083	S0096
Similarity Score	764	810	680	708

III. IMPACT OF SPUTTER COATING ON 3D TARGET FEATURES

Following the sputter deposition of Ti and Au on the physical 3D targets, we perform fidelity assessment of friction ridge etchings on the gold fingers. To conduct the fidelity experiments, we generate four different 3D targets by projecting different fingerprints (S0005, S0010, S0083, S0096) from NIST SD4 [34] onto a 3D finger surface [7]. Two of these

[6]In contrast, the diameter of a human hair is an order of magnitude thicker (typically between 17-181 μm [32]).

[7]The fingerprints in NIST SD4 are rolled ink-on-paper impressions.

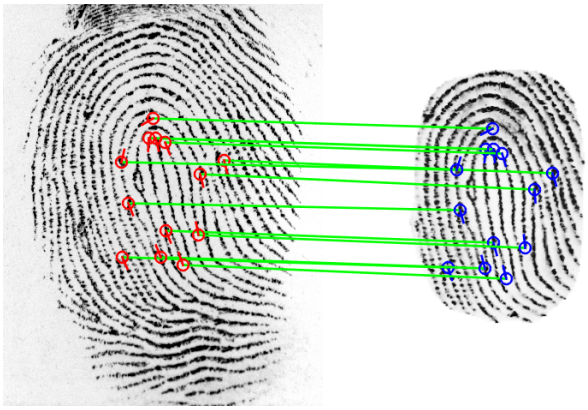

Fig. 8. Minutiae correspondence between (a) plain impression of the 3D target generated using fingerprint image S0083 from NIST SD4 captured by the optical reader, and (b) plain impression of the gold finger post sputter depositing the same target captured by the capacitive reader (a). Similarity score of 680 is obtained between (a) and (b) which is above the threshold of 33 at 0.01% FAR.

TABLE V
SIMILARITY SCORES BETWEEN PLAIN IMPRESSIONS OF THE SPUTTER COATED GOLD FINGERS CAPTURED USING 500 PPI CAPACITIVE READER TO THE CORRESPONDING 2D FINGERPRINTS FROM NIST SD4 USED IN THEIR GENERATION. VERIFINGER 6.3 [33] WAS USED FOR GENERATING SIMILARITY SCORES. THE THRESHOLD ON SCORES @FAR = 0.01% IS 33.

Source Fingerprint (NIST SD4)	S0005	S0010	S0083	S0096
Similarity Score	471	333	183	203

targets (S0005, S0010) are fabricated with TangoBlackPlus FLX980 [13], and the other two (S0083 S0096) are fabricated with FLX 9840-DM [14]. There is a reduction in etching spacings on physical 3D targets compared to ground truth due to 2D to 3D projection of calibration pattern (5.8%) and 3D printing (11.42%) [17]. To compensate for this reduction, we set the scale while projecting the 2D calibration pattern to 16.79 pixels/mm. This a priori projection scale adjustment ensures that spacings in the original 2D calibration patterns are maintained in the 3D target etchings post 2D to 3D projection and 3D printing. Finally, the depth between ridges and valleys on the 3D targets is set to 0.24 mm.

A commercial 500 ppi *Appendix F* certified optical reader[8] is used to capture plain impressions of the physical 3D targets, whereas a commercial 500 ppi *PIV* certified capacitive reader is used for capturing the plain impressions of the gold fingers. Verifinger 6.3 [33], a commercially available fingerprint SDK, is used for fingerprint comparison.

A. Fidelity of physical 3D target features on gold fingers

Plain impressions of the physical 3D targets captured using the optical reader before sputter coating are compared to the plain impressions of the corresponding gold finger captured using the capacitive reader after sputter deposition. This comparison of pre and post sputter deposition target images is used to assess how well the features on the physical 3D targets (e.g. ridge spacing and minutiae) are preserved on gold fingers after sputter deposition. Table IV shows the comparison results of this experiment. The similarity scores obtained for all comparisons are significantly above the verification threshold score of 33 computed for NIST SD4 at a fixed false accept rate (FAR) of 0.01%. This indicates that the physical 3D target features are replicated with high fidelity on the gold fingers.

[8]The make and model of the readers used in the experiments cannot be disclosed because of proprietary reasons.

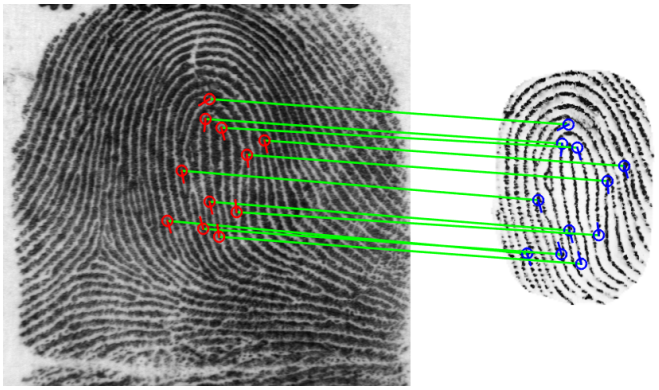

Fig. 9. Minutiae correspondence between (a) rolled fingerprint image S0083 from NIST SD4, and (b) plain impression of the gold finger generated using (a) captured by the capacitive reader. Similarity score of 183 is obtained between (a) and (b) which is above the threshold of 33 at 0.01% FAR.

TABLE VI
RANGE OF SIMILARITY SCORES BETWEEN FIVE DIFFERENT 500 PPI PLAIN IMPRESSIONS OF EACH SPUTTER COATED GOLD FINGER CAPTURED BY THE CAPACITIVE READER. VERIFINGER 6.3 [33] WAS USED FOR GENERATING SIMILARITY SCORES. THE THRESHOLD ON SCORES @FAR = 0.01% IS 33.

Source Fingerprint (NIST SD4)	S0005	S0010	S0083	S0096
Score Range	926-1251	884-1164	824-1215	462-1008

B. Fidelity of 2D calibration pattern features on gold fingers

Plain impressions of the gold fingers captured using the capacitive reader are compared to the corresponding 2D fingerprint images from NIST SD4 used in their generation. End-to-end fidelity of 2D calibration pattern features on gold fingers is assessed based on how well the 2D pattern features are replicated on the gold fingers. Table V shows the comparison results. For all comparisons, the similarity scores generated are above the verification threshold score of 33 for NIST SD4 at FAR of 0.01%. This demonstrates that the 2D calibration pattern features were replicated with high fidelity on the gold fingers.

C. Intra-class variability between impressions of gold fingers

Five different plain impressions of each gold finger are captured using the capacitive reader and compared against each other in order to assess the consistency between different impressions of the same gold finger. Table VI shows the range of similarity scores obtained for this experiment. All similarity scores are significantly higher than the verification threshold

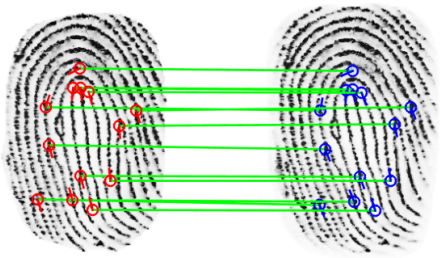

Fig. 10. Minutiae correspondence between two different plain impressions (a) and (b) of the same gold finger (S0083 from NIST SD4) captured by the capacitive reader. Similarity score of 1164 is obtained between (a) and (b) which is above the threshold of 33 at 0.01% FAR.

TABLE VII
MEAN (μ) AND STD. DEVIATION (σ) OF CENTER-TO-CENTER RIDGE SPACING (IN PIXELS) IN THE IMAGES OF THE GOLD FINGERS CAPTURED USING THE 500 PPI SINGLE-FINGER CAPACITIVE READER (CR). MEASURED RIDGE SPACING (IN PIXELS) IN THE CORRESPONDING ORIGINAL FINGERPRINT IS SHOWN IN BRACKETS.

Source Fingerprint (NIST SD4)	**CR (500 ppi)**
S0005 (9.45)	μ = 9.57, σ = 0.14
S0010 (10.20)	μ = 10.34, σ = 0.21
S0083 (10.44)	μ = 10.60, σ = 0.14
S0096 (10.24)	μ = 10.28, σ = 0.11

score of 33 for NIST SD4 at FAR of 0.01%. This shows that different impressions of the same gold finger are highly consistent. In other words, the intra-class variability between different impressions of the same gold finger is very small.

IV. EVALUATION OF CAPACITIVE READERS

We evaluate (i) a large area (~1.3 cm×1.8 cm) *PIV* certified 500 ppi standalone reader and (ii) small area (~0.5 cm×0.9 cm) capacitive readers embedded in smartphones using gold fingers.

A. Large area capacitive reader

Five different plain impressions of each gold finger are captured with the capacitive reader (see, e.g., Fig. 11). The center-to-center ridge spacing in each captured impression is measured by counting the number of pixels between two consecutive gray level intensity peaks along the direction perpendicular to the ridge flow [35]. The average measured ridge spacing from the five impressions of each gold finger is compared to the ridge spacing of the corresponding original fingerprint (computed using the same method [35]) used in the design of the gold finger. Table VII shows the average and standard deviation in ridge spacing measured from the five impressions. Following are the key observations based on this experiment:

- The computed ridge spacing in images of all four gold fingers is, on average, within 0.15 pixels of the measured spacing in the corresponding original fingerprint. This is most likely due to the flattening of gold finger gratings when they are pressed against the capacitive reader platen, and is consistent with our earlier observation based on contact-based optical readers. Using the one-sample t-test [36], the difference between the computed ridge spacing and the measured original spacing is statistically significant at 0.05 significance level. Note, however, that the increase in ridge spacing observed here is not as large as that reported with optical readers [17]. To better understand these differences, controlled experimentation with known contact pressure during fingerprint capture is required.
- The average deviation in ridge spacing between different impressions of the same gold finger is between 0.1 to 0.2 pixels. These are comparable to the ridge spacing deviation measurements obtained for 3D targets using one of the optical readers, but slightly larger than spacing measurements reported previously for the other two optical readers [17]. This can be explained by the capacitive reader having a smaller platen compared to the two optical readers which only partially images the gold fingers. Therefore, overall fewer ridge spacing measurements are used for spacing computations.

B. Small area embedded readers

Experiments are performed using two different smartphones, the Apple iPhone 6s and the Samsung Galaxy S7[9], and a stand-alone small area capacitive reader module designed for smartphones. Fig. 7 shows the impressions acquired with capacitive reader module designed for smartphones. We first enroll a gold finger using the fingerprint enrollment procedure on the two smartphones and the capacitive reader module as shown in Fig. 12 (a). Subsequently, we make ten independent attempts to unlock the two phones and the capacitive reader module using the enrolled gold finger. The enrolled gold finger template is then deleted and we repeat this procedure using a different gold finger. We were able to successfully unlock the two phones and the capacitive reader module in every attempt using each of the four gold fingers (see Fig. 12 (b)). This indicates the potential feasibility of using gold fingers as targets for evaluating capacitive readers embedded in smartphones.

V. PRESENTATION ATTACKS ON CAPACITIVE READERS

Artifically generated 2D fingerprint artifacts have been previously used for perfomring presentation attacks (spoofing) on capacitive readers [37] [38]. Although the primary goal of fabricating conductive 3D fingerprint artifacts (gold fingers) is evaluation of capacitive readers, a significant by-product of this research is the potential use of such artifacts in performing presentation attacks on capacitive readers. Sputter coating 3D printed artifacts to create high fidelity gold fingers requires specialized equipment and materials (a sputtering system, and titanium and gold sputtering targets) that are generally not easily available. However, a simple alternative procedure using

[9]Commercial smartphones do not provide access to fingerprint images used for enrollment and subsequent unlocking.

(a) (b) (c) (d) (e)

Fig. 11. Five different impressions of a gold finger captured using the large area *PIV* certified capacitive reader. The center-to-center ridge spacing measurements in each impression are used for the evaluation of the reader.

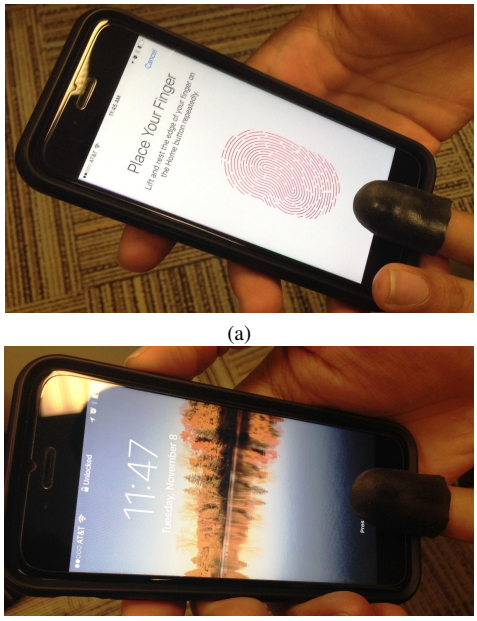

(a)

(b)

Fig. 12. Evaluation of capacitive readers embedded in smartphones using gold fingers. (a) Enrollment of a gold finger on an Apple iPhone 6s, and (b) unlocking of the iPhone 6s using the same gold finger.

off-the-shelf conductive carbon coating described below can be used to create a conductive 3D spoof from a 2D plain fingerprint impression of a known subject (Fig. 13).

1) **Design electronic spoof:** Use a 3D modeling software, e.g, Meshlab [29], to synthetically generate a cuboidal surface for projecting the 2D fingerprint. Set the length and width of the cuboid to at least 3.5 cm and 2.5 cm, respectively. This ensures that there is adequate surface area for projecting the fingerprint. The height (wall thickness) of the cuboid needs to be atleast 1 mm for 3D printing the cuboid as a solid object. The electronic 3D spoof is created by etching the 2D fingerprint onto the cuboidal surface [18]. While creating the electronic spoof, set the 2D to 3D projection scale appropriately (16.79 pixels/mm) to account for 2D to 3D projection error and 3D printing fabrication error.
2) **Fabricate the physical spoof:** Fabricate the 3D spoof using a high-resolution 3D printer (e.g. Stratasys Objet Connex350) with materials similar in hardness and elasticity to the human skin (e.g. TangoBlackPlus FLX980) [17].
3) **Clean the physical spoof:** Dip the 3D printed spoof in 2M NaOH solution for approx. 3 hrs. and then rinse it with water. Let it dry after cleaning procedure.
4) **Coat the spoof with conductive coating:** Spray coat conductive carbon (e.g. [39]) onto the cleaned spoof. This imparts the required conductivity for registering the spoof on capacitive readers[10].

We generated five 3D spoofs from index fingerprints of five different subjects using the aforementioned procedure. The spoofs were fabricated with TangoBlackPlus FLX980. Note that unlike wearable 3D fingerprint targets, the 3D spoofs are not wearable. To image a spoof, it is placed on a capacitive reader and a slight pressure is applied on top of it (see Fig. 14). For conducting spoofing experiments, the index fingerprints of the subjects were enrolled on two different capacitive readers, a single-finger capacitive reader and an embedded capacitive reader in an access control terminal. Verfinger 6.3 SDK was interfaced with the single-finger capacitive reader for performing fingerprint comparisons. For the embedded reader, the fingerprint comparison algorithm built into the access control terminal was used for fingerprint comparisons. Five separate spoofing attempts were made on each of the readers using the five spoofs. In all attempts, we were able to successfully spoof the two readers.

Although the generated 3D spoofs were able to spoof a single-finger standalone reader and an embedded reader in an access control terminal, they were unable to spoof capacitive readers embedded in smartphones. We believe this is because fingerprint comparison algorithms in smartphones primarily use texture-based features. Small area readers in smartphones capture images ($\sim 70 \times 120$ pixels) that typically contain only a few minutia points; in some cases, the captured images may not even contain a single minutia (see Fig. 7). Given that the texture characteristics of the created 3D spoofs differ from the human skin, these spoofs are not effective for capacitive readers in smartphones.

[10]Spray coating of conductive carbon is non-uniform. Furthermore, the carbon coating only imparts conductivity for a limited time (1-2 hours), and has low abrasion resistance. This process, therefore, cannot be used for creating conductive 3D targets.

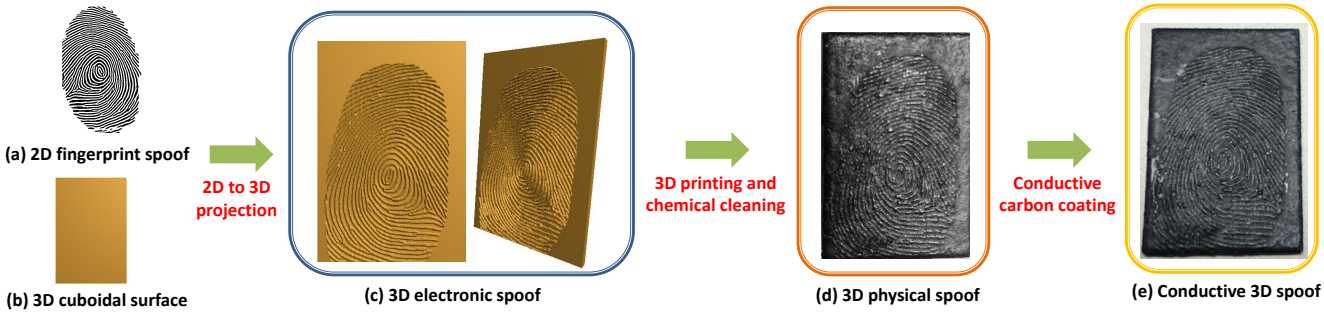

Fig. 13. Main steps involved in creating a conductive 3D spoof given a 2D fingerprint of a known subject and a 3D cuboidal surface. (a)-(c) The 2D fingerprint is projected onto the cuboidal surface to generate a 3D electronic spoof and (d) 3D physical spoof is fabricated from the electronic spoof in (c) using a high-resolution 3D printer [17]. (e) Conductive carbon is spray coated on the 3D physical spoof to generate the conductive 3D spoof.

(a) (b) (c) (d)

Fig. 14. Spoofing a capacitive reader embedded in an access control terminal using a conductive 3D spoof created from a fingerprint of a known subject. (a) The fabricated conductive 3D spoof, (b) the spoof is placed on the reader platen, (c) pressure is applied on top of the spoof, and (d) successfully spoofing of the reader on the access control terminal (facility door is unlocked).

VI. Conclusions and Future Work

Capacitive fingerprint readers are now being increasingly used in consumer and access control applications, e.g., for smartphone unlock and point of sale (POS) payments. Given the widespread deployment of capacitive readers, an important requirement is to develop standard artifacts and procedures for repeatable evaluation of these readers. We have described a procedure to design and fabricate conductive 3D targets by applying a thin layer of conductive material coating (titanium and gold) on 3D printed physical targets for capacitive reader evaluation. The resulting conductive 3D targets are called gold fingers. We demonstrate that the 2D calibration patterns and the corresponding features (e.g., minutiae) can be replicated with high fidelity on the gold fingers. We show that the gold fingers can be used as targets for testing capacitive readers embedded in smartphones as well as a capacitive reader used for access control. The spoof vulnerability of commercially available capacitive readers to presentation attacks using 3D printed spoofs is also assessed.

Because gold fingers do not work well with optical readers due to high surface reflectivity post gold coating, we plan to explore methods to design and build a universal 3D target with both the optical and the electrical properties similar to human skin. This would facilitate benchmarking of different optical and capacitive readers, as well as investigation of reader inter-operability using the same 3D targets. We will also conduct additional evaluation experiments (e.g. to test the resolution of capacitive readers) using gold fingers. Additionally, we would like to study how user-induced variabilities, such as the contact-pressure applied on the reader platen and relative finger distortion, impact the quality of the captured fingerprint images. To do this, controlled experimentation where known contact-pressure is applied on the reader platen while capturing fingerprint impressions will be performed. We also plan to develop anti-spoofing solutions to prevent presentation attacks using 3D printed spoofs.

Acknowledgments

This research was supported by grant no. 60NANB11D155 from the NIST Measurement Science program. The authors would like to thank Brian Wright, Michigan State University, and Matthew Staymates, National Institute of Standards and Technology, for their assistance with 3D printing of fingerprint targets. We would also like to thank Brian Wright, Chris Traverse, Dr. Richard Lunt, and Lars Haubold, Michigan State University for their help in sputter coating the 3D printed targets with different conductive materials.

References

[1] "TechTarget Smartphone definition," http://searchmobilecomputing.techtarget.com/definition/smartphone.
[2] "Statista: Number of smartphone users worldwide from 2014 to 2019," http://www.statista.com/statistics/330695/number-of-smartphone-users-worldwide/.

[3] "Statista: Penetration of smartphones with fingerprint sensors from 2014 to 2018," http://www.statista.com/statistics/522058/global-smartphone-fingerprint-penetration/.
[4] "Statista: NFC mobile payment users worldwide from 2012 to 2018," http://www.statista.com/statistics/461512/nfc-mobile-payment-users-worldwide/.
[5] "TouchID System," http://support.apple.com/kb/ht5949.
[6] "Samsung Fingerprint Sensor," http://www.samsung.com/us/support/answer/ANS00039905/997339942/SM-G920TZKATMB.
[7] "Google Nexus," https://www.google.com/nexus/.
[8] D. Maltoni, D. Maio, A. Jain, and S. Prabhakar, *Handbook of Fingerprint Recognition*. Springer, 2009.
[9] C. Edwards and R. Marks, "Evaluation of biomechanical properties of human skin," *Clinics in Dermatology*, vol. 13, no. 4, pp. 375–380, 1995.
[10] V. Falanga and B. Bucalo, "Use of a durometer to assess skin hardness," *Journal of the American Academy of Dermatology*, vol. 29, no. 1, pp. 47–51, 1993.
[11] Y. A. Chizmadzhev, A. V. Indenbom, P. I. Kuzmin, S. V. Galichenko, J. C. Weaver, and R. O. Potts, "Electrical properties of skin at moderate voltages: contribution of appendageal macropores," *Biophysical Journal*, vol. 74, no. 2, pp. 843–856, 1998.
[12] G. K. Johnsen, "Skin electrical properties and physical aspects of hydration of keratinized tissues," Ph.D. dissertation, University of Oslo, 2010.
[13] "Stratasys Polyjet Material Data Sheet," http://www.stratasys.com/~/media/Main/Secure/Material%20Specs%20MS/PolyJet-Material-Specs/PolyJet_Materials_Data_Sheet.pdf.
[14] "Stratasys Digital Materials (DMs) Data Sheet," http://www.stratasys.com/~/media/Main/Secure/Material%20Specs%20MS/PolyJet-Material-Specs/Digital_Materials_Datasheet.pdf.
[15] N. B. Nill, "Test procedures for verifying image quality requirements for personal identity verification (PIV) single finger capture devices," MITRE, Tech. Rep. MTR 060170, 2006.
[16] ——, "Test procedures for verifying IAFIS image quality requirements for fingerprint scanners and printers v 1.4," MITRE, Tech. Rep. MTR 05B0016R7, 2013.
[17] S. S. Arora, K. Cao, A. K. Jain, and N. G. Paulter Jr., "Design and Fabrication of 3D Fingerprint Targets," *IEEE Transactions on Information Forensics and Security*, vol. 11, no. 10, pp. 2284–2297, 2016.
[18] S. S. Arora, A. K. Jain, and N. Paulter Jr., "3D Whole Hand Targets: Evaluating Slap and Contactless Fingerprint Readers," in *International Conference of the Biometrics Special Interest Group (BIOSIG)*, 2016.
[19] T. Swain, "Vacuum Technology 60A & 60B: Thin Film Deposition Processes," http://lpc1.clpccd.cc.ca.us/lpc/tswain/chapt14.pdf.
[20] "Denton Vacuum Desktop Pro Sputtering System," http://www.dentonvacuum.com/technologies/production-solutions/desktop-pro/.
[21] "Stratasys Objet Connex350," https://www.egr.msu.edu/eceshop/testingfacility/connex/index.php.
[22] K. Seshan, *Handbook of Thin Film Deposition*. William Andrew, 2012.
[23] M. Boehme and C. Charton, "Properties of ITO on PET film in dependence on the coating conditions and thermal processing," *Surface and Coatings Technology*, vol. 200, no. 1, pp. 932–935, 2005.
[24] D. Cho, K. Kim, T. Kim, Y. Noh, S. Na, K. Chung, and H. Kim, "Transparent and flexible amorphous InZnAlO films grown by roll-to-roll sputtering for acidic buffer-free flexible organic solar cells," *Organic Electronics*, vol. 24, pp. 227–233, 2015.
[25] H. Im, H. Hong, J. Lee, J. Lee, Y. Heo, and J. Kim, "Structural and electrical properties of al and b co-doped zno thin films," *Journal of Nanoelectronics and Optoelectronics*, vol. 6, no. 3, pp. 301–305, 2011.
[26] C. A. Bishop, "Transparent Conducting Coatings on Polymer Substrates for Touchscreens and Displays," in *Handbook of Visual Display Technology*. Springer, 2012, pp. 975–988.
[27] T. Takano, H. Masunaga, A. Fujiwara, H. Okuzaki, and T. Sasaki, "PEDOT nanocrystal in highly conductive PEDOT:PSS polymer films," *Macromolecules*, vol. 45, no. 9, pp. 3859–3865, 2012.
[28] D. Alemu, H. Wei, K. Ho, and C. Chu, "Highly conductive PEDOT: PSS electrode by simple film treatment with methanol for ito-free polymer solar cells," *Energy & Environmental Science*, vol. 5, no. 11, pp. 9662–9671, 2012.
[29] "Meshlab," http://sourceforge.net/projects/meshlab/.
[30] "Kurt J. Lesker Gold (Au) Sputtering Targets," http://www.lesker.com/newweb/deposition_materials/depositionmaterials_sputtertargets_1.cfm?pgid=au1.
[31] "Kurt J. Lesker Titanium (Ti) Sputtering Targets," http://www.lesker.com/newweb/deposition_materials/depositionmaterials_sputtertargets_1.cfm?pgid=ti1.
[32] "Diameter of a Human Hair," http://hypertextbook.com/facts/1999/BrianLey.shtml.
[33] Neurotechnology Inc. Verifinger, http://www.neurotechnology.com/verifinger.html.
[34] "NIST Special Database 4," http://www.nist.gov/srd/nistsd4.cfm.
[35] L. Hong, Y. Wan, and A. K. Jain, "Fingerprint image enhancement: algorithm and performance evaluation," *IEEE Transactions on Pattern Analysis and Machine Intelligence*, vol. 20, no. 8, pp. 777–789, 1998.
[36] D. S. Moore, *The Basic Practice of Statistics*. WH Freeman, 2007, vol. 2.
[37] T. Matsumoto, H. Matsumoto, K. Yamada, and S. Hoshino, "Impact of artificial gummy fingers on fingerprint systems," in *Electronic Imaging*. International Society for Optics and Photonics, 2002, pp. 275–289.
[38] J. Galbally, J. Fierrez, F. Alonso-Fernandez, and M. Martinez-Diaz, "Evaluation of direct attacks to fingerprint verification systems," *Telecommunication Systems*, vol. 47, no. 3-4, pp. 243–254, 2011.
[39] "Total Ground Carbon Conductive Coating," http://www.unicornelex.com/ProductDetails.asp?ProductCode=26-0801&gclid=CN7Nh5qmv88CFQMdaQodkNMNNA.

Sunpreet S. Arora received the B.Tech. (Hons.) degree in Computer Science from the Indraprastha Institute of Information Technology, Delhi (IIIT-D) in 2012, and the Ph.D. degree in Computer Science and Engineering from Michigan State University, East Lansing in 2016. He is currently a Senior Biometrics Researcher at Visa Inc., Foster City, CA. His research interests include biometrics, pattern recognition and image processing. He received the best paper award at the 15th International Conference of the Biometrics Special Interest Group (BIOSIG), 2016, and the best poster award at the IEEE Fifth International Conference on Biometrics: Theory, Applications and Systems (BTAS), 2012. He is a student member of the IEEE.

Anil K. Jain is a University distinguished professor in the Department of Computer Science and Engineering at Michigan State University. He is a Fellow of the ACM, IEEE, IAPR, AAAS and SPIE. His research interests include pattern recognition and biometric authentication. He served as the editor-in-chief of the IEEE Transactions on Pattern Analysis and Machine Intelligence, a member of the United States Defense Science Board and the Forensics Science Standards Board. He has received Fulbright, Guggenheim, Alexander von Humboldt, and IAPR King Sun Fu awards. He is a member of the United States National Academy of Engineering and a Foreign Fellow of the Indian National Academy of Engineering.

Nicholas G. Paulter Jr. is the Group Leader for the Security Technologies Group at NIST in Gaithersburg, MD. He develops and oversees metrology programs related to concealed weapon and contraband imaging and detection, biometrics for identification, and body armor characterization. He has authored or co-authored over 100 peer-reviewed technical articles and provided numerous presentations at a variety of technical conferences. He is a 2008-2009 Commerce Science and Technology Fellow and a 2010 IEEE Fellow.